Committee of the Royal Society and the University of London Research Funds Committee, who provided much of the X-ray equipment.

References

BJURSTRÖM, T. (1933). *Ark. Kemi Min. Geol.* A, **11**, No. 5.
BOOTH, A. D. (1947). *Nature, Lond.* **160**, 196.
BRADLEY, A. F. (1935). *Proc. Phys. Soc.* **47**, 879.
BUDDERY, J. H. & WELCH, A. J. E. (1951). *Nature, Lond.* **167**, 362.
KIESSLING, R. (1950). *Acta chem. Scand.* **4**, 209.
PAULING, L. (1947). *J. Amer. Chem. Soc.* **69**, 542.
PAULING, L. (1949). *Proc. Roy. Soc.* A, **196**, 343.
TOMAN, K. (1952). *Acta Cryst.* **5**, 329.

Acta Cryst. (1954). **7**, 53

On the Structure of Epidote

BY T. ITO, N. MORIMOTO AND R. SADANAGA*

Mineralogical Institute, University of Tokyo, Hongo, Tokyo, Japan

(*Received* 19 *March* 1953)

The structure of epidote, $HCa_2(Al, Fe)Al_2Si_3O_{13}$, has been refined by two- and three-dimensional syntheses. The revised structure, in favour of which an earlier proposal was withdrawn, has now been confirmed. The structure is of the mixed silicate type containing both SiO_4 and Si_2O_7 groups bound together by Al, Al(Fe), Ca and O atoms and OH groups. Epidote is an alumino-silicate, like cyanite etc., as the Al and O atoms and OH groups form octahedral chains which occupy the bulk of its structure.

Introduction

One of the present writers several years ago proposed for epidote a structure (Ito, 1947) which was later abandoned in favour of another structure (Ito, 1950, p. 50). The latter structure should be preferred, we argued, because it was better able to derive the structure of the closely related mineral, zoisite. As far as the agreement between calculation and the experimental data then available was concerned, however, a different conclusion might have been drawn (Evans, 1952), and indeed our aim was rather to illustrate the usefulness of the concept of polysymmetric synthesis in dealing with a certain class of polymorphic crystals. We give below an account of our later work undertaken to determine the structure more precisely.

Experimental

In addition to those used in the previous studies, a great many further experimental data were accumulated. The *h*0*l* reflexions observed on the ionization spectrometer (Ito, 1950, p. 54) were checked and supplemented by the data obtained photographically, correcting in particular those weak reflexions which were hard to measure accurately with the spectrometer. Relative intensities estimated visually in the *b*(0) Weissenberg photographs (Mo and Co $K\alpha$) were correlated with the absolute values and incorporated into the *h*0*l* spectra. Together with these, the evaluated reflexions deduced from the *a*(0, 1, 3), *b*(1, 2) (Co $K\alpha$) and *b*(3, 4, 5) (Mo $K\alpha$) Weissenberg–Buerger photographs and rendered absolute (Harker, 1948; $B = 1{\cdot}0 \times 10^{-16}$ cm.^{2}) cover practically the whole reciprocal space ordinarily observable and form the bulk of the experimental information on which the present study is based.

The photographs were processed by the multiple-film technique (Lange, Robertson & Woodward, 1938). For the intensities of reflexions only the Lorentz and polarization factors were taken into account, no correction for absorption or extinction having been made.

The specimens examined were the same as those used previously (Prince of Wales Island, Alaska), having an almost ideal composition of $HCa_2FeAl_2Si_3O_{13}$ (Ito, 1950, p. 51). The unit cell has the dimensions

$$a = 8{\cdot}96,\ b = 5{\cdot}63,\ c = 10{\cdot}30\ \text{Å},\ \beta = 115°\ 24',$$

and contains four units of the above formula. The space group is $P2_1/m$, the reflexions 0*k*0 being absent when *k* is odd.

Refinement by the Patterson–Harker functions

Our previous analysis was based on the finding that the *y* coordinates of all the atoms in epidote are 0, $\frac{1}{4}$, $\frac{1}{2}$ or $\frac{3}{4}$. This was derived by considering the peculiarity of the 0*k*0 reflexions and the geometry of the lattice with reference to the size of the constituent ions. Quite generally, the *b*(*n*) and *b*(*n*+4) Weissenberg–Buerger photographs display a virtually identical intensity distribution. This is possible in space group

* Temporarily at Chemistry Department, University College, London W.C. 1, England.

$P2_1/m$ only when the atoms occupy the above-mentioned positions.

Should the atoms really be in such special positions the set of four Harker functions $P(u, 0, w)$, $P(u, \frac{1}{4}, w)$, $P(u, \frac{1}{2}, w)$ and $P(u, \frac{3}{4}, w)$, being tantamount to the complete Patterson function $P(u, v, w)$, would be the most useful instrument for testing the structure conceived. However, since these functions proved to be insufficiently simple to supply immediate information we transformed them into a form more convenient to interpret. First, we combined two Harker diagrams, $P(u, 0, w)$ and $P(u, \frac{1}{2}, w)$ (Fig. 1(*a*), (*b*)), by superposing them on the xz plane and taking point by point the *lesser* value. The resulting minimum function may be considered to represent the interactions of atoms exclusively on $(010)_0$, for the process eliminates largely those on other levels and also those between different levels. We designate it $P'(u, 0, w)$ (Fig. 1(*c*)).

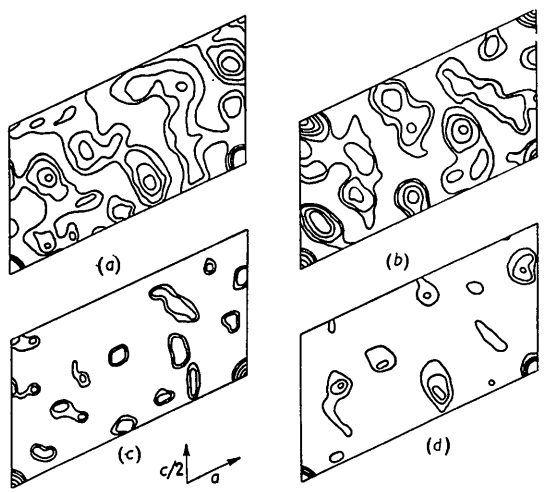

Fig. 1. Vector maps. (*a*) $P(u, 0, w)$. (*b*) $P(u, \frac{1}{2}, w)$. (*c*) $P'(u, 0, w)$. (*d*) $P'(u, \frac{1}{4}, w)$. (See text.)

A similar function $P'(u, \frac{1}{4}, w)$ that expresses the interactions of atoms solely on the $(010)_{\frac{1}{4}}$ level was then obtained by taking the *difference* point by point, again on the xz plane, between the corresponding values of $P(u, 0, w)$ and $P'(u, 0, w)$ (Fig. 1(*d*)). We need consider only these two reduced Patterson–Harker functions, as the interactions on other levels are the same as these on account of the space-group symmetry. We can now readily single out on the vector diagrams derived in this way a combination of possible positions, especially of metal ions, which evidently support our revised structure. Accordingly, we first adjusted the positions of the metal atoms until they conformed to the vector maps. In re-locating oxygen atoms around the metal atoms the usual packing relations and coordination were taken into account. The new parameters are compared with the original ones in Table 1, columns (1) and (2).

Further refinement by the two-dimensional Fourier synthesis

For the summation of the double series the Beevers–Lipson strips were used. The a and c axes were each subdivided into 60 parts, giving intervals of 0·15 and 0·17 Å. The first summation was carried out using 38 observed F_{h0l}'s whose signs were determined with certainty by the new parameters. With the parameters further successively refined, the second summation was made with 52, the third with 115, the fourth with 225 and the fifth with 240 terms (all not counting terms with the zero intensity). We give in Fig. 2 the

Table 1. *Coordinates of atoms*

Atom	No. of atoms in the cell	x/a (1)	x/a (2)	x/a (3)	x/a (4)	y/b (1)	y/b (4)	z/c (1)	z/c (2)	z/c (3)	z/c (4)
Si_1	2	0·35	0·360	0·342	0·342	0·75	0·750	0·06	0·067	0·057	0·055
Si_2	2	0·70	0·710	0·681	0·682	0·25	0·250	0·30	0·287	0·272	0·270
Si_3	2	0·20	0·224	0·189	0·183	0·75	0·750	0·30	0·334	0·313	0·314
Al_1	2	0	0	0	0	0	0	0	0	0	0
Al_2	2	0	0	0	0	0	0	0·50	0·500	0·500	0·500
Al(Fe)	2	0·27	0·304	0·297	0·297	0·25	0·250	0·21	0·226	0·226	0·227
Ca_1	2	0·76	0·750	0·755	0·755	0·75	0·750	0·15	0·154	0·145	0·150
Ca_2	2	0·60	0·610	0·603	0·603	0·750	0·750	0·45	0·415	0·422	0·421
O_1	4	0·24	0·234	0·232	0·235	0	0·992	0·03	0·063	0·053	0·053
O_2	4	0·32	0·324	0·303	0·300	0	0·978	0·35	0·380	0·347	0·353
O_3	4	0·76	0·800	0·798	0·798	0	0·008	0·40	0·360	0·342	0·338
O_4*	2	0·06	0·060	0·047	0·047	0·25	0·250	0·15	0·144	0·138	0·142
O_5	2	0·06	0·060	0·047	0·047	0·75	0·750	0·15	0·144	0·138	0·142
O_6	2	0·06	0·064	0·082	0·080	0·75	0·750	0·40	0·400	0·413	0·413
O_7	2	0·50	0·500	0·523	0·522	0·75	0·750	0·20	0·200	0·187	0·183
O_8	2	0·45	0·525	0·517	0·530	0·25	0·250	0·20	0·300	0·315	0·315
O_9	2	0·72	0·650	0·620	0·625	0·25	0·250	0·15	0·100	0·100	0·098
OH	2	0·06	0·064	0·082	0·080	0·25	0·250	0·40	0·400	0·413	0·413

* Not directly bonded to Si.

(1) See Ito (1950, p. 53).
(2) Values by the Patterson–Harker synthesis.
(3) Values by the two-dimensional synthesis.
(4) Final values by the three-dimensional synthesis.

result of the sixth and final synthesis (again made with 240 terms), in which the maxima coincide with the atomic positions chosen (see Table 1, column (3)).

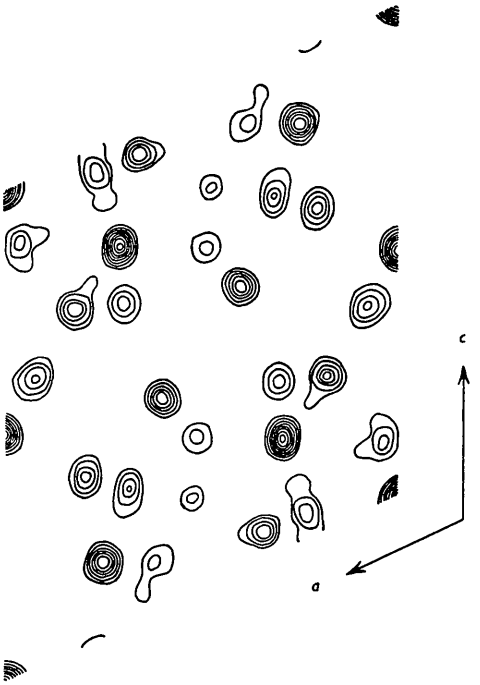

Fig. 2. Fourier projection of electron density on (010). Contours at intervals of 5 e.Å^{-2}, zero lines being omitted.

Final determination by the three-dimensional synthesis

The double synthesis thus gave a well-defined map of electron density which permitted a precise reading of the x and z coordinates. Since, however, the y coordinates were summarily assumed at the outset it was deemed desirable that they be confirmed more directly. Calculating about one thousand F_{hkl}'s and using the observed F_{hkl}'s ($Q_{hkl} = 4\sin^2\theta/\lambda^2 < 1{\cdot}45$ Å^{-2}) with the signs as calculated, the triple series were summed up thus:

$$\varrho(x, 0, z) = \frac{1}{V}\Big[\sum_h\sum_l\Big\{\sum_k F_{hkl}\Big\}\cos 2\pi hx \cos 2\pi lz - \sum_h\sum_l\Big\{\sum_k F_{hkl}\Big\}\sin 2\pi hx \sin 2\pi lz\Big];$$

$$\varrho(x, \tfrac{1}{4}, z) = \frac{1}{V}\Big[\sum_h\sum_l\Big\{\sum_k F_{hkl}\cos 2\pi k/4\Big\}\cos 2\pi hx \cos 2\pi lz - \sum_h\sum_l\Big\{\sum_k F_{hkl}\cos 2\pi k/4\Big\}\sin 2\pi hx \sin 2\pi lz - \sum_h\sum_l\Big\{\sum_k F_{hkl}\sin 2\pi k/4\Big\}\cos 2\pi hx \sin 2\pi lz - \sum_h\sum_l\Big\{\sum_k F_{hkl}\sin 2\pi k/4\Big\}\sin 2\pi hx \cos 2\pi lz\Big].$$

In the synthesis the a and c edges were each subdivided as earlier into 60 parts and the electron density of the (010) sections at $y = 0$ and $y = \frac{1}{4}$ was evaluated. We give in Fig. 3 the composite Fourier diagram in which the contours of the two sections are superimposed.

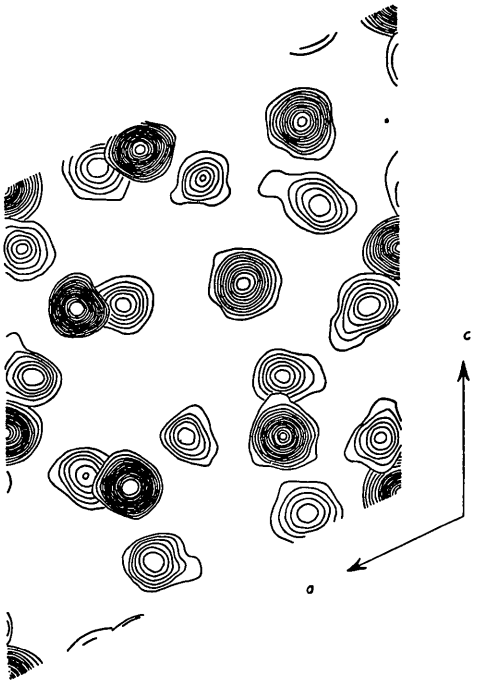

Fig. 3. Composite diagram of the Fourier sections, $(010)_0$ and $(010)_{\frac{1}{4}}$, of electron density. Contours at intervals of 2 e.Å^{-3}, zero lines being omitted.

Although the result of the synthesis necessitated still further slight shifts of atomic positions to arrive at the final values of the x and z coordinates (the shifts did not occasion any change of signs of the calculated F_{hkl}'s), the contours on the diagram are concentrated almost exactly where anticipated and the density peaks are for the most part of the height consistent with the electron configuration of the atoms concerned. This indicates that the $(010)_0$ and $(010)_{\frac{1}{4}}$ sections cut right through the centres of the individual atoms, justifying the postulate we set up initially.

On the other hand, the oxygen atoms placed on $(010)_0$, namely O_1, O_2 and O_3, unlike oxygen and other atoms on $(010)_{\frac{1}{4}}$ which is a reflexion plane, are not symmetry-bound and might be situated appreciably above or below the plane. Actually the peaks on the diagram that delineate the positions of these oxygen atoms are a little lower than they should be, being less than 12 e.Å^{-3} instead of the usual 13 e.Å^{-3}.

In order to ascertain their possible shifts the summation of the triple series,

$$\varrho(p, y, q) = \frac{1}{V}\Big[\sum_k\Big\{\sum_h\sum_l F_{hkl}\cos 2\pi(hp+lq)\Big\}\cos 2\pi ky - \sum_k\Big\{\sum_h\sum_l F_{hkl}\sin 2\pi(hp+lq)\Big\}\sin 2\pi ky\Big],$$

was carried out at the points $p = 0.235$, $q = 0{\cdot}053$;

Table 2. *Comparison of observed and calculated F_{hkl}-values*

hkl	F_o	F_c	*hkl*	F_o	F_c	*hkl*	F_o	F_c
001	6	− 4	4,0,$\bar{11}$	34	−35	10,0,$\bar{5}$	38	30
002	18	−19	4,0,$\bar{12}$	—	−14	10,0,$\bar{6}$	15	12
003	31	30	4,0,$\bar{13}$	—	19	10,0,$\bar{7}$	20	7
004	19	22	4,0,$\bar{14}$	30	10	10,0,$\bar{8}$	12	2
005	21	9				10,0,$\bar{9}$	50	47
006	35	12	500	26	12	10,0,$\bar{10}$	23	32
007	28	11	50$\bar{1}$	10	−18	10,0,$\bar{11}$	—	1
008	7	2	50$\bar{2}$	86	76	10,0,$\bar{12}$	41	47
009	20	9	50$\bar{3}$	34	30			
0,0,10	10	12	50$\bar{4}$	25	−16	11,0,0	—	− 3
0,0,11	55	62	50$\bar{5}$	17	− 3	10,0,$\bar{1}$	—	1
0,0,12	31	38	50$\bar{6}$	59	51	11,0,$\bar{2}$	33	34
0,0,13	10	7	50$\bar{7}$	14	−10	11,0,$\bar{3}$	—	25
0,0,14	37	35	50$\bar{8}$	10	−19	11,0,$\bar{4}$	—	− 9
0,0,15	7	4	50$\bar{9}$	12	10	11,0,$\bar{5}$	32	−21
			5,0,$\bar{10}$	36	46	11,0,$\bar{6}$	22	32
100	32	9	5,0,$\bar{11}$	8	4	11,0,$\bar{7}$	29	−30
10$\bar{1}$	28	24	5,0,$\bar{12}$	60	62	11,0,$\bar{8}$	—	−19
10$\bar{2}$	57	61	5,0,$\bar{13}$	—	2	11,0,$\bar{9}$	60	53
10$\bar{3}$	16	− 9	5,0,$\bar{14}$	—	−14	11,0,$\bar{10}$	49	46
10$\bar{4}$	40	50	5,0,$\bar{15}$	5	6			
10$\bar{5}$	41	38				12,0,0	21	12
10$\bar{6}$	121	125	600	34	28	12,0,$\bar{1}$	—	10
10$\bar{7}$	41	35	60$\bar{1}$	12	−17	12,0,$\bar{2}$	22	25
10$\bar{8}$	14	5	60$\bar{2}$	15	16	12,0,$\bar{3}$	—	3
10$\bar{9}$	18	2	60$\bar{3}$	62	46	12,0,$\bar{4}$	11	4
1,0,$\bar{10}$	55	52	60$\bar{4}$	127	104	12,0,$\bar{5}$	—	4
1,0,$\bar{11}$	10	11	60$\bar{5}$	47	−43	12,0,$\bar{6}$	11	− 9
			60$\bar{6}$	17	10	12,0,$\bar{7}$	34	41
200	71	−63	60$\bar{7}$	23	−17	12,0,$\bar{8}$	6	24
20$\bar{1}$	12	− 4	60$\bar{8}$	40	64	12,0,$\bar{9}$	72	−77
20$\bar{2}$	54	64	60$\bar{9}$	13	− 2	12,0,$\bar{10}$	11	5
20$\bar{3}$	18	3	6,0,$\bar{10}$	5	− 4			
20$\bar{4}$	18	−20	6,0,$\bar{11}$	38	42	13,0,0	29	38
20$\bar{5}$	29	20	6,0,$\bar{12}$	9	− 2	13,0,$\bar{1}$	40	−38
20$\bar{6}$	53	−46	6,0,$\bar{13}$	—	− 3	13,0,$\bar{2}$	—	− 3
20$\bar{7}$	20	18	6,0,$\bar{14}$	24	−26	13,0,$\bar{3}$	—	− 1
20$\bar{8}$	69	71				13,0,$\bar{4}$	60	52
20$\bar{9}$	61	−40	700	11	8			
2,0,$\bar{10}$	81	77	70$\bar{1}$	22	16	14,0,0	18	−13
2,0,$\bar{11}$	20	26	70$\bar{2}$	7	2	14,0,$\bar{1}$	—	14
2,0,$\bar{12}$	34	35	70$\bar{3}$	25	18	14,0,$\bar{2}$	—	−10
			70$\bar{4}$	42	35	14,0,$\bar{3}$	—	− 2
300	92	90	70$\bar{5}$	21	1	14,0,$\bar{4}$	13	14
30$\bar{1}$	19	18	70$\bar{6}$	5	1			
30$\bar{2}$	58	64	70$\bar{7}$	24	−25	101	25	−19
30$\bar{3}$	21	−15	70$\bar{8}$	60	56	102	59	53
30$\bar{4}$	27	27	70$\bar{9}$	28	30	103	13	− 6
30$\bar{5}$	37	−41	7,0,$\bar{10}$	90	69	104	29	−29
30$\bar{6}$	90	−89	7,0,$\bar{11}$	7	− 7	105	50	−59
30$\bar{7}$	25	−21	7,0,$\bar{12}$	—	−21	106	22	−15
30$\bar{8}$	112	100	7,0,$\bar{13}$	—	1	107	9	2
30$\bar{9}$	28	23	7,0,$\bar{14}$	52	51	108	86	79
3,0,$\bar{10}$	32	−23				109	13	5
3,0,$\bar{11}$	12	− 8	900	12	6	1,0,10	12	− 2
3,0,$\bar{12}$	11	3	90$\bar{1}$	26	−13	1,0,11	—	21
3,0,$\bar{13}$	—	−12	90$\bar{2}$	35	25	1,0,12	45	40
3,0,$\bar{14}$	30	34	90$\bar{3}$	39	35			
3,0,$\bar{15}$	9	7	90$\bar{4}$	60	61	201	62	−53
			90$\bar{5}$	14	10	202	91	101
400	75	69	90$\bar{6}$	25	28	203	83	71
40$\bar{1}$	111	116	90$\bar{7}$	25	14	204	45	33
40$\bar{2}$	25	−25	90$\bar{8}$	37	35	205	10	8
40$\bar{3}$	44	30	90$\bar{9}$	26	40	206	64	69
40$\bar{4}$	27	−14	9,0,$\bar{10}$	24	32	207	52	45
40$\bar{5}$	24	−23				208	25	−21
40$\bar{6}$	120	124	10,0,0	51	43	209	43	37
40$\bar{7}$	15	−25	10,0,$\bar{1}$	60	−61	2,0,10	50	48
40$\bar{8}$	38	17	10,0,$\bar{2}$	7	9			
40$\bar{9}$	13	11	10,0,$\bar{3}$	49	43	301	16	36
4,0,$\bar{10}$	38	38	10,0,$\bar{4}$	48	43	302	18	11

Table 2 (*cont.*)

hkl	F_o	F_c	*hkl*	F_o	F_c	*hkl*	F_o	F_c
303	30	−31	505	59	−43	707	20	−13
304	73	58	506	44	39	708	30	15
305	83	63	507	60	59			
306	22	15				801	12	− 6
307	7	−13	601	22	24	802	52	50
308	15	19	602	29	−26	803	19	15
309	30	−29	603	49	31	804	12	− 6
			604	36	26	805	33	37
401	23	−23	605	22	−22	806	17	24
402	13	− 8	606	77	51	807	—	15
403	57	−54	607	50	−48	808	37	30
404	83	55	608	26	−18			
405	—	0	609	7	10	901	55	50
406	38	27	6,0,10	42	39	902	43	34
407	6	− 2				903	8	− 3
408	49	53	701	45	−45	904	—	5
			702	20	−19	905	—	−24
501	5	− 3	703	48	−35	906	36	32
502	82	74	704	83	64			
503	11	8	705	31	30	10,0,1	30	−34
504	5	− 7	706	—	15	10,0,2	35	−26

$p = 0{\cdot}300$, $q = 0{\cdot}353$ and $p = 0{\cdot}798$, $q = 0{\cdot}338$, where they are seen in projection. The result revealed that the maxima of electron density along [010] (Fig. 4)

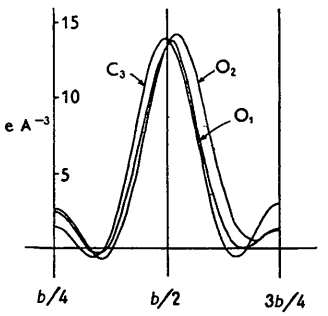

Fig. 4. Electron density along [010].

are located in positions which deviate slightly but significantly from zero. The y coordinates of these oxygen atoms were corrected accordingly and were regarded as final as they involved no further change of sign of the calculated F_{hkl}'s.

The final atomic coordinates are given in Table 1, column (4). They are considered to be probably accurate to 0·03 Å for O and to 0·01 Å for Al, Al(Fe), Ca and Si. In Table 2 we list the observed F_{h0l}'s contrasted with the F_{h0l}'s calculated on the basis of these coordinates. The reliability number $R\ (=\Sigma||F_o|-|F_c||\div\Sigma|F_o|)$ is 0·218 for *h0l* reflexions and 0·275 for the *hkl* reflexions, all (*c.* 1000) present and absent reflexions being counted.

The structure redescribed

The refined structure of epidote is illustrated in Fig. 5. No correction or modification of the general terms in which the structure was originally described (Ito, 1950, p. 64) is necessary.

The structure is of the mixed silicate type, con-

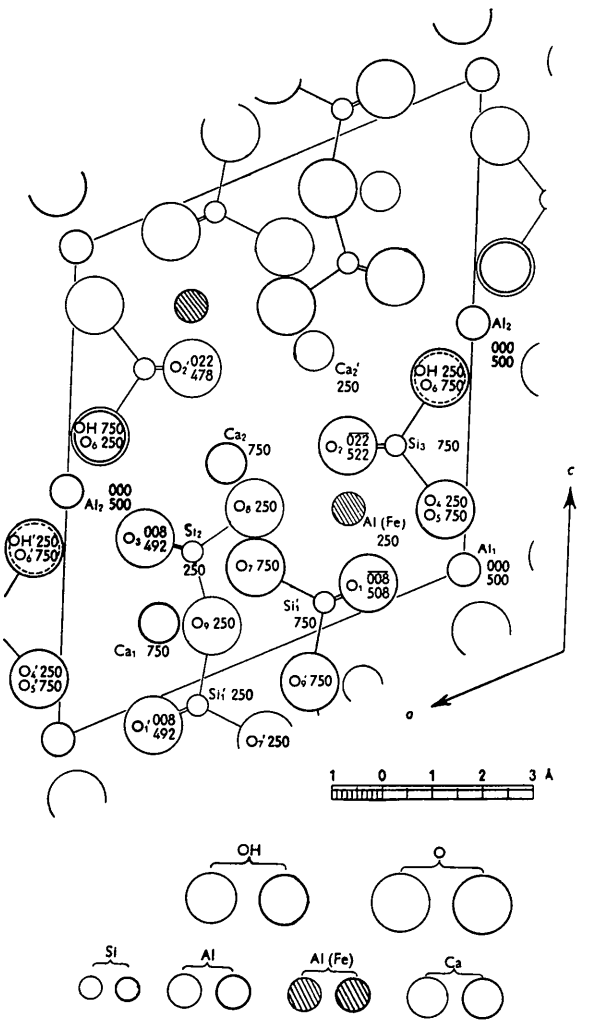

Fig. 5. The structure of epidote projected on (010) (cf. Figs. 2 and 3). The numbers give the height of each atom from (010) as a permilliage of the b length. SiO_4 and Si_2O_7 groups are indicated.

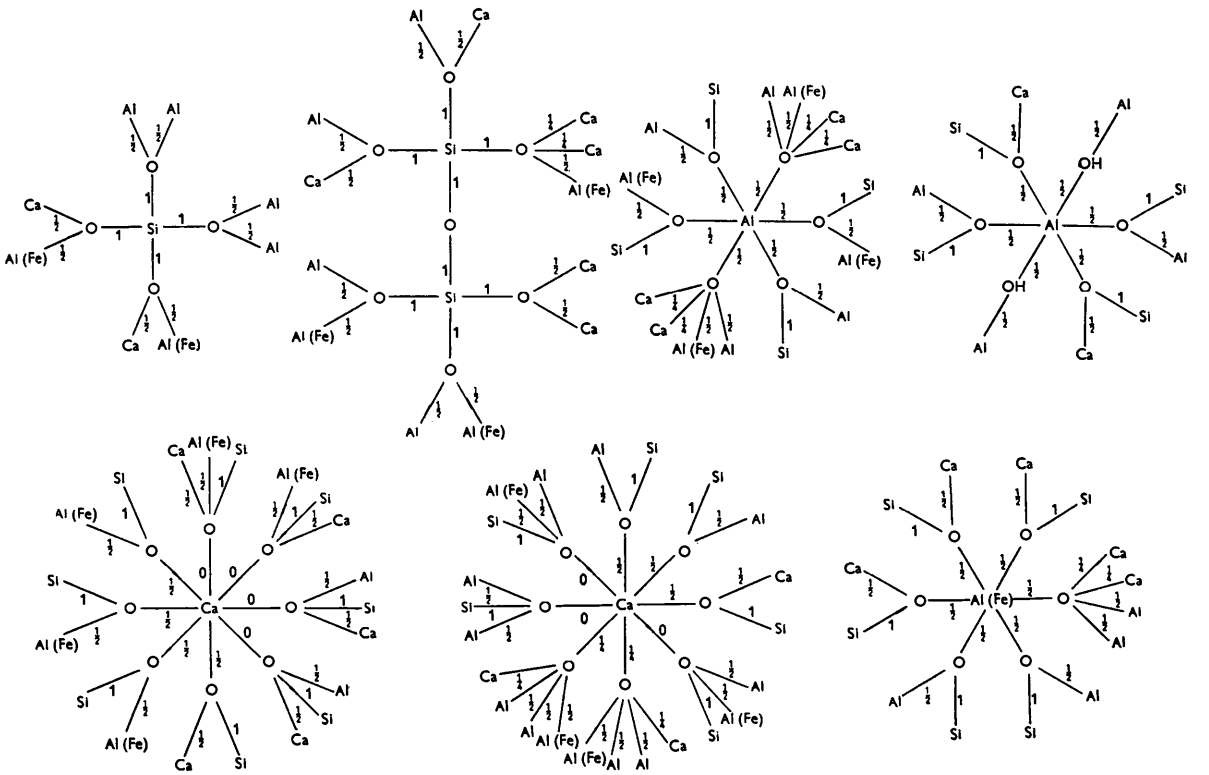

Fig. 6. Electrostatic balance of bonds around metal atoms in epidote.

Table 3. *Interatomic distances*

Atom	Neighbour	Distance (Å)
Si_1	O_1 (2)	1·66
	O_7	1·59
	O_9'	1·70
Si_2	O_3 (2)	1·65
	O_8	1·61
	O_9	1·60
Si_3	O_2 (2)	1·60
	O_5	1·66
	O_6	1·63
Al_1	O_1 (2)	1·94
	O_4 (2)	1·94
	O_5 (2)	1·94
Al_2	O_3 (2)	1·86
	O_6 (2)	1·96
	OH (2)	1·96
Al(Fe)	O_1 (2)	2·15
	O_2 (2)	2·01
	O_4	2·01
	O_8	1·89
Ca_1	O_1'(2)	2·51*
	O_3 (2)	2·30
	O_4'(2)	3·34
	O_5'	2·65*
	O_7	2·25
Ca_2	O_2 (2)	2·80*
	O_2'(2)	2·55
	O_3 (2)	2·66*
	O_7	2·22
	O_8	2·98
O_1	O_1	2·72
	O_2	2·86
	O_4	2·66
	O_4'	2·80
	O_5	2·60
	O_5'	2·88
	O_7	2·62
	O_8	3·18
	O_9'	2·64
O_2	O_6	2·64
O_3	O_3	2·72
	O_6	2·72
	O_6'	2·66
	O_8	2·60
	O_9	2·56
	OH	2·68
	OH′	2·71
O_4	O_5	2·82
	O_5'	2·65
O_5	O_6	2·67
O_6	OH	2·82
	OH′	2·71
O_7	O_9'	2·58
O_8	O_9	2·69

* Not bonded to the central atom.

taining both the single- and double-tetrahedral groups, SiO_4 and Si_2O_7. These separate groups are joined to one another by Al, Al(Fe) and Ca atoms on the one hand and by O atoms and OH groups on the other. Al atoms are surrounded octahedrally either by six O atoms or by five O atoms and one OH group. Al(Fe) atoms, too, have an octahedral coordination. Ca atoms are eightfold coordinated by O atoms in a rather irregular fashion.

In an alternative description, as also given pre-

viously, emphasis might be laid on the Al–O and Al–O–OH linkages rather than on the Si–O linkage. The framework of the structure consists of the AlO_4 and AlO_3OH chains which are similar in shape to those found in cyanite and other alumino-silicate minerals (see Bragg, 1937). The chains are formed by O and O–OH octahedra around Al holding the O–O edges in common. They are stretched parallel to each other and to the *b* axis and are bound together sidewise by Al(Fe), Ca and Si atoms, each of which is oxygen-coordinated as mentioned above.

The chemical analysis of epidote (see for example, Dana, 1900) has invariably demonstrated that the atomic ratio Fe:Al is no more than 1:2. This may be explained if we recognize the fact that Fe atoms do not replace Al atoms of the chains.

The balance of valency is illustrated in Fig. 6 and the interatomic distances are given in Table 3. It is to be noted that they have been considerably improved by the present refinement.

References

BRAGG, W. L. (1937). *The Atomic Structure of Minerals.* Ithaca: Cornell University Press.

DANA, E. S. (1900). *The System of Mineralogy,* 6th ed., p. 519. New York: Wiley.

EVANS, H. T. (1952). *Acta Cryst.* **5**, 297. (Book review.)

HARKER, D. (1948). *Amer. Min.* **33**, 764.

ITO, T. (1947). *Amer. Min.* **32**, 309.

ITO, T. (1950). *X-ray Studies in Polymorphism.* Tokyo: Maruzen.

LANGE, J. J. DE, ROBERTSON, J. M. & WOODWARD, I. (1939). *Proc. Roy. Soc.* A, **171**, 398.

Acta Cryst. (1954). **7**, 59

On the Shape of Cylindrical Patterson Function Peaks*

BY HARRY L. YAKEL, JR.

Gates and Crellin Laboratories of Chemistry, California Institute of Technology, Pasadena 4, California, U.S.A.

(*Received* 21 *April* 1953 *and in revised form* 7 *July* 1953)

In the course of an investigation of cylindrical Patterson functions as applied to the structures of fibrous polypeptides, the shape function for Gaussian distributions surrounding interatomic vectors in three-dimensional Patterson space projected cylindrically about a unique axis has been determined. This shape function is the Patterson space analogue of an electron distribution function in real space. The projected shape function is such that for the large temperature and disorientation factors associated with fibrous polypeptides there are significant deviations in both peak location and size from an ordinary Patterson projection.

An approach to the deduction of the structures of fibrous proteins and synthetic polypeptides from their X-ray diffraction diagrams lies in the calculation and interpretation of cylindrical Patterson projections for these substances. Such functions were first described by MacGillavry & Bruins (1948), and have recently been calculated for poly-γ-methyl-L-glutamate and collagen (Yakel & Schatz, to be published). In the interpretation of these projections, it proved desirable to compare the experimental results with Patterson functions calculated from the distribution of interatomic vectors for one or more suggested models of the folded polypeptide chain. Simple comparison of the observed functions with maps containing the interatomic vectors represented by suitably weighted points yielded little information, presumably owing to the poor resolution of the observed functions caused by limited data and large temperature and disorientation factors. An attempt was therefore made to obtain a mathematical expression for the shape of the peaks in cylindrical Patterson projections which would contain variable parameters depending on temperature factor, etc. It was hoped that a more representative picture of what might be expected in the experimental projections could then be derived from the theoretical shape functions.

It can be shown that a three-dimensional Patterson peak shape function, $P_{ij}(r)$, may be defined by the equation

$$P_{ij}(r) = 4\pi \int_0^\infty f_i f_j \cdot \frac{\sin 2\pi r H}{2\pi r H} \cdot H^2 . dH \,, \qquad (1)$$

where f_i and f_j are the atomic scattering factors of the two atoms involved in the interaction, H equals $2 \sin \theta/\lambda$, and r is a radial coordinate measured from the end of the interatomic vector between atoms i and j in Patterson space, as indicated in Fig. 1. The function $P_{ij}(r)$ may be identified with a distribution func-

* Contribution No. 1800 from the Gates and Crellin Laboratories. This work was supported by Contract NOnr 220 (5) between the California Institute of Technology and the Office of Naval Research.